FRACTURE BEHAVIOUR OF FERRITIC AND AUSTENITIC STEEL PIPES

H. ZEIBIG, F. FORTMANN

INTERATOM, Internationale Atomreaktorbau GmbH, D-506 Bensberg/Köln, Germany

SUMMARY

The paper describes recent developments in the analysis of ferritic and austenitic structural materials provided for use in the design of the liquid metal fast breeder reactors KNK II and SNR.

To prove the integrity of the primary systems, a fracture mechanics approach is used to define the critical crack-tip stress conditions for rapid failure and fatigue crack propagation. The experiments were conducted with through-wall flawed specimens of the original pipes used in the loop of the KNK-reactor and with specimens of the same wall thickness as provided for use in SNR.

In continuing previous work two pipes of 10CrMoNiNb910 steel with artificial circumferential cracks were tested, one with the crack located in the welded zone.

The austenitic specimens were made from No. 1.4948 steel, which is similar to the Type AISI 304 steel provided for the Fast Flux Test Facility (FFTF).

Two pipes with axial flaws and two pipes with circumferential flaws, one of which was located in the welded zone, were tested at room temperatures. These specimens were subjected to fluctuating internal pressure prior to the rupture test, thus getting real conditions at the crack-tip and information on the fatigue crack propagation.

The experimental results are compared with new calculations based on fracture mechanics. They are in good agreement with the theoretical predictions for critical flaw sizes and fatigue crack propagation rates. The results of fatigue crack propagation drawn from measurements on austenitic specimens are in agreement with experimental results of other investigations with flat plates.

The investigations do not show any indications that unstable fracture would be possible under operational conditions, both for the ferritic and the austenitic steel used in the design of KNK II and SNR. Compared with the wall thickness, the critical crack lengths are so large that failures will manifest themselves by leaking prior to fracture.

1. INTRODUCTION

Further investigations were made in order to demonstrate that instable fracture is improbable in the primary systems of the LMFBR's KNK II and SNR.

The experiments were carried out in nearly the same manner as described in [1]. Two additional tests with circumferential cracks, one of which was located in the welded joint, were made with 10 CrMoNiNb 910 steel pipes.

The austenitic specimens were made from 1.4948 steel, which is similar to the Type AISI 304 steel. Two pipes with axial flaws and two pipes with circumferential flaws, one of which was located in the welded joint, were tested at room temperature. The paper includes results of four tests with axial flaws of the same steel and the same dimensions [2].
The specimens were subjected to fluctuating internal pressure prior to the rupture test, thus giving real conditions at the crack-tip and providing information on the fatigue crack propagation.

2. NOTATION

K_c - critical stress intensity factor
D_m - mean diameter
R_m - mean radius
t - wall thickness
c - half crack length
σ_h - hoop stress at failure
σ_y - yield stress
σ_u - ultimate stress
σ^* - flow stress, Ref. [4]
M - stress magnification factor
ν - Poisson's ratio

3. THROUGH-WALL CRACK FORMULATIONS

To discuss the experimental results, two crack formulations were used. The critical stress intensity factor K_c for axial and circumferential cracks (under mode I conditions) given by F. ERDOGAN and M. RATWANI [3] reads as follows

$$K_c = \sigma_h \sqrt{\pi c}\,(A_m \pm A_b) \qquad (1)$$

The stress intensity ratios or curvature correction factors A_m and A_b contribute to the membrane and bending loads of the cylindrical shell under internal pressure only. In the case of a flat plate $A_b = 0$ and $A_m = 1$. The plus and the minus signs in equation (1) denote the outer and inner surface, respectively. At the middle of the wall-thickness the bending term vanishes.

HAHN et al. [4] proposed a formulation for axial cracks only which includes a flow stress criterion for the material.
The stress intensity factor is given by

$$K_c = \sigma^{\times} \left[\frac{8c}{\pi} \ln \sec \frac{\pi}{2} \frac{M \sigma_n}{\sigma^{\times}} \right] \qquad (2)$$

In both equations all the relevant shell dimensions enter into the stress magnification factors A_m, A_b and M only through the parameter

$$\lambda = \left[12 (1 - \nu^2) \right]^{1/4} \frac{c}{\sqrt{Rt}} \qquad (3)$$

4. RESULTS

A summary of experimental and calculated results for the ferritic and austenitic pipes is given in tables 1 and 2. In the calculations the lowest values of the hoop stress at crack initiation are used.
Figure 1 shows a graph of equation (1) along with the data points from the experiments for the ferritic steel pipes. The K_c-values neglecting the influence of the bending loads (i.e. $A_b = 0$) give the best fit with regard to the experiments. The deformations in the vicinity of the crack are comparatively large, thus reducing obviously the bending factor A_b.

At the same hoop stress, the critical crack lengths for circumferential cracks are much larger than for axial cracks. This is in agreement with the theory which gives lower stress magnification factors for circumferential cracks than for axial cracks [3].

Figure 2 shows the graph of equations (1) and (2) along with the data points from the experiments for the 1.4948 steel pipes. The critical crack lengths for the circumferential cracks are also much larger than for axial cracks.

The agreement with the experimental data points is surprisingly good.

For higher hoop stresses, equation (1) is no more in agreement with the experiments, because it contains no flow stress criterion. At a certain K_c-value and $c \rightarrow 0$, the hoop stress tends to infinity.

The experiments on the austenitic specimens were carried out using pipes of the actual wall thickness as provided for SNR, but with a smaller diameter. For the actual diameter of the SNR loops the curve of hoop stress σ_n against critical length is seen in figure 3, calculated from equation (2) keeping the K_c-value constant. The actual radius leads to greater critical crack lengths. This is in agreement with the theory which gives the greatest values for the flat plate.

Because of the decreasing flow stress with increasing temperatures, the curve changes to lower critical crack length at operating temperatures, as can be seen from figure 3.

Prior to the burst tests the specimens were pressure-cycled, so getting fatigue crack-growth data and real crack tip conditions for the burst tests.

Figure 4 shows the crack-growth data obtained with the four circumferential and axial cracks of the austenitic pipes. They are compared with experiments [5] on flat plate single-edge-notch (SEN) and wedge-opening-load (WOL) type specimens at room and elevated temperatures. The agreement is rather good.

5. CONCLUSION AND REMARKS

The results of the experimental investigations on reactor piping specimens for use in the LMFBR's KNK II and SNR, with axial and circumferential through - wall cracks, are in good agreement with the theoretical predictions for critical flaw sizes and crack growth rates. They also agree with experimental results of other investigations [5].

At operating conditions, the stress levels of the KNK II and SNR piping systems are in the range of 40 to 60 N/mm^2. Thus the critical crack lengths are considerable with regard to the wall-thickness.

Furthermore there are no critical crack depths in the systems, as can be shown by the following equation [6]

$$\left(\frac{a}{Q}\right)_{cr} = \frac{1}{1.21\pi}\left(\frac{K_{Ic}}{\sigma}\right)^2 \qquad (4)$$

where a denotes the critical crack depth and Q the crack form parameter. K_{Ic} is the lowest stress intensity factor measured at plane strain conditions.

For thin-walled pipes where plane stress conditions exist - as can be seen from figures 5 and 6 - the lowest stress intensity factor is the K_c factor at crack initiation measured on specimens with the actual wall-thickness.

Regarding an infinite crack length and making the conservative assumption that the hoop stress σ_h is nearly as high as the yield stress σ_y, Q becomes 0.788. With $(K_c/\sigma_y)^2 > 400$ in table 2 one gets the critical crack depth to be about 80 mm. This value is much larger than the wall-thickness anywhere in the systems. Hence it is safe to say that no sudden rupture can occur.

Moreover the crack growth behaviour can be computed, using the curve at operating temperatures from reference [5]. Assuming an initial crack of 20 mm length, about 10^3 cycles between 0 and 100 N/mm^2 are necessary to increase the crack to a length of 20.3 mm.

In general, it was found that the fracture mechanics concept is able to describe the fracture behaviour of the ferritic and austenitic steels provided for use in the LMFBR's KNK II and SNR. There is no indication that unstable fracture would be possible under operational conditions. The crack growth behaviour - if actually significant - can only lead to leakages.

REFERENCES

/_1_/ ZEIBIG, H. and FORTMANN, F., "Fracture Behaviour Investigations of 10CrMoNiNb910 Steel Pipes", Proc. First Int. Conf. on Structural Mech. in Reactor Technology, Vol. 6-Part L, Berlin, Germany, 20-24 Sept. 1971

/_2_/ HENRY, B. et al., "Fatigue Crack Growth in Austenitic Stainless Steel Structures", paper to be published at the 2nd Int. Conf. on Structural Mech. in Reactor Technology, Berlin, Germany 10-14 Sept. 1973

/_3_/ ERDOGAN, F. and RATWANI, M., "Fracture of Cylindrical and Spherical Shells Containing a Crack", Techn. Report NASA-TR-71-3, Juli 1971

/_4_/ HAHN, G.T. et al., "Criteria for Crack Extension in Cylindrical Pressure Vessels", Int. J. of Fracture Mech., Vol. 5, 1969

/_5_/ JAMES, L.A. and SCHWENK, JR.E.B., "Fatigue-Crack Propagation Behaviour of Type 304 Stainless Steel at Elevated Temperatures", Metallurgical Transactions, Vol. 2, 1971

/_6_/ TIFFANY, C.F. and MASTERS, J.N., "Fracture Toughness Testing and its Applications", ASTM Spec. Techn. Publ. No. 381, 1965

Table 1. Summary of Experimental and Calculated Results for 10CrMoNiNb910 Steel Pipes

Exp. No.	Crack Orientation+)	D_m mm	t mm	c mm	σ_y N/mm^2	σ_u N/mm^2	σ_n N/mm^2	λ -	Kc, Eq. (1) N · mm$^{-3/2}$
1	A++)	210.0	8.3	124.5			67.6	7.67	5732
2	A++)	210.2	8.0	225.8			36.3	14.14	6866
3	A++)	212.2	7.9	59.6	266	492	214.9	3.74	7350
								average	6649
4	C	211.0	8.0	185.0			71.2	11.58	4121
5	C_w	209.8	8.3	142.5			130.8	8.78	5674

+) A axial crack, C circumferential crack, C_w circumferential crack, welded joint
++) Ref. [1]

Table 2. Summary of Experimental and Calculated Results for 1.4948 Steel Pipes (Type AISI - 304)

Exp. No.	Crack Orientation+)	D_m mm	t mm	c mm	σ_y N/mm^2	σ_u N/mm^2	σ_h N/mm^2	λ --	Kc Eq.(1) N · mm$^{-3/2}$	Kc Eq.(2) N · mm$^{-3/2}$
1	A++)	344.2	9.8	13.3	206	576	289.4	0.59	-	-
2	A++)	344.2	9.8	28.0			194.8	1.24	-	3006
3	A++)	343.6	10.4	53.1			160.6	2.28	-	5180
4	A++)	344.5	9.5	111.4			76.0	5.0	-	5023
5	A	343.5	9.9	135.1	210	547	57.8	5.96	4227	4592
6	A++)	343.9	10.1	200.5	206	576	42.1	8.74	-	5601
7	A	343.2	10.3	205.2	210	547	31.0	8.88	3778	3987
							average		4003	4565
8	C	343.6	9.9	99.4	304	576	118.0	4.39	3128	
9	C_w	341.1	11.1	258.4	304	576	70.1	10.80	4494	

+) A axial crack, C circumferential crack, C_w circumferential crack, welded joint
++) Ref. [2]

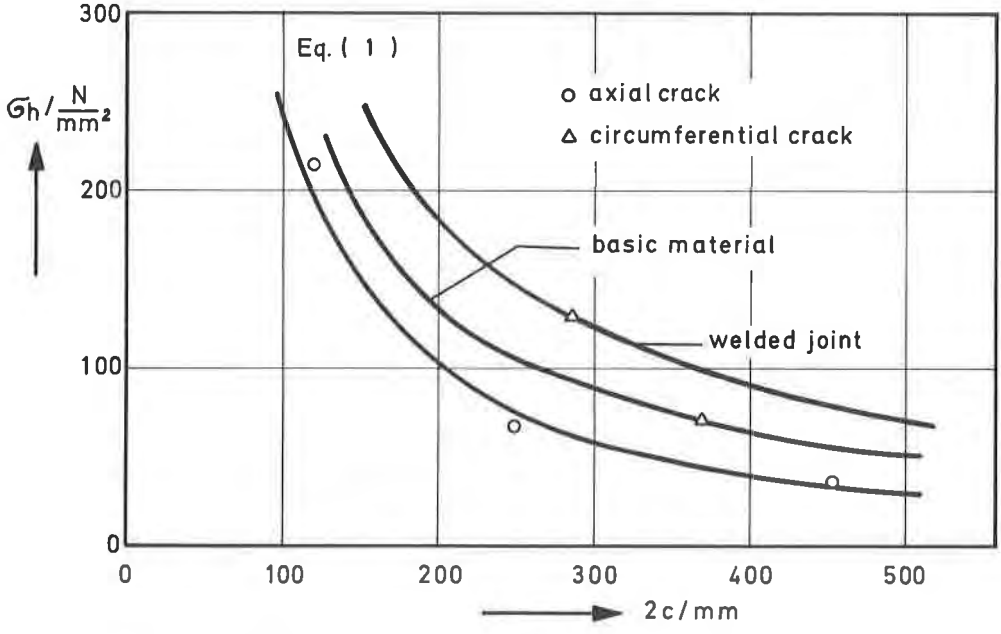

FIGURE 1: Failure stress curves and experimental data on 10CrMoNiNb910 steel pipes.

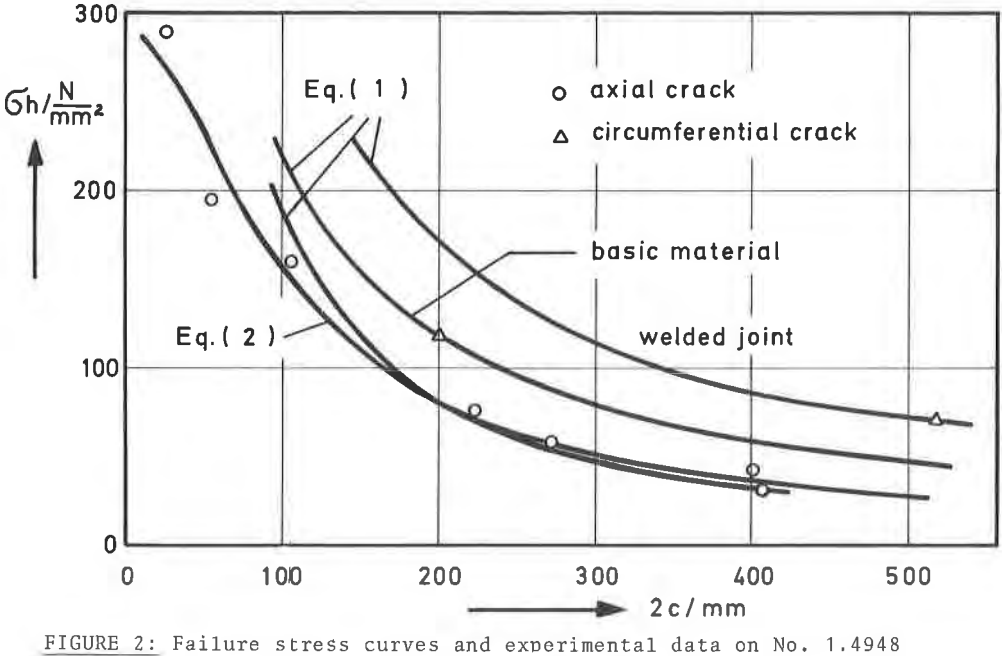

FIGURE 2: Failure stress curves and experimental data on No. 1.4948 (Type AISI 304) steel pipes.

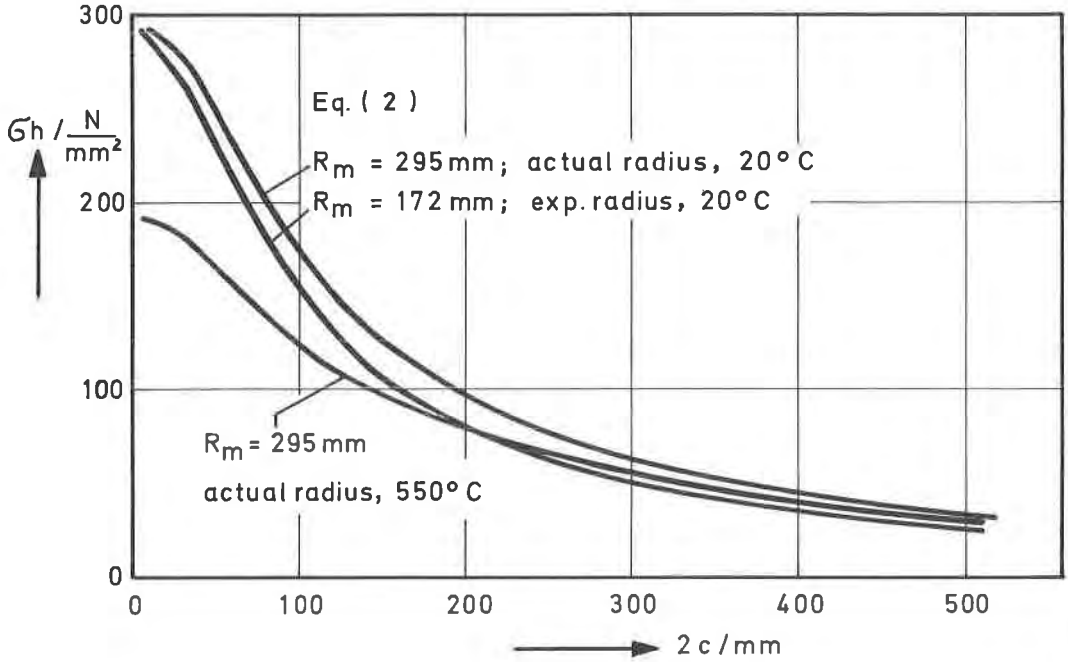

FIGURE 3: Failure stress curves calculated for the actual radius of No. 1.4948 (Type AISI 304) steel pipes.

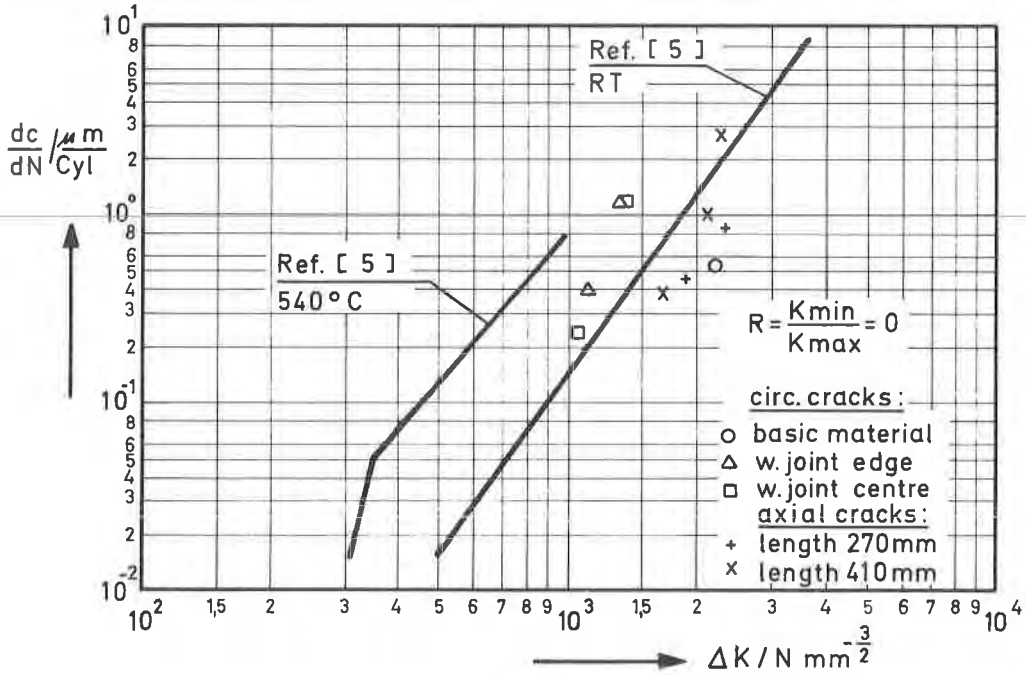

FIGURE 4: Crack growth rates of No. 1.4948 (Type AISI 3o4) steel pipes. Comparison with data from ref. [5].

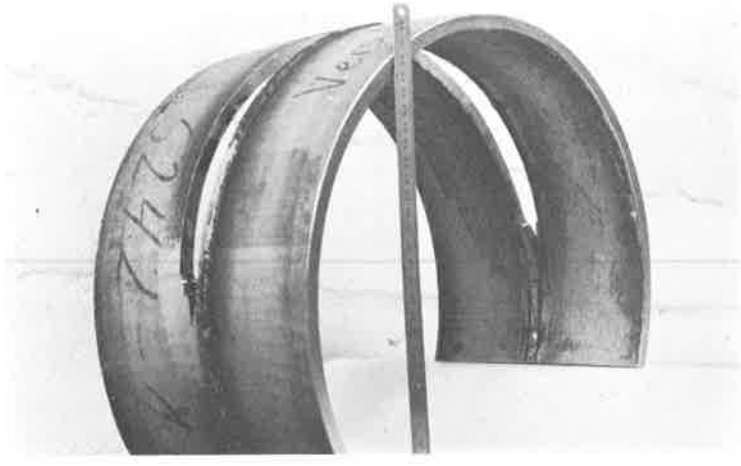

FIGURE 5: Pipe section with circumferential crack at the welded joint after being cracked. No. 1.4948 (Type AISI 304) steel.

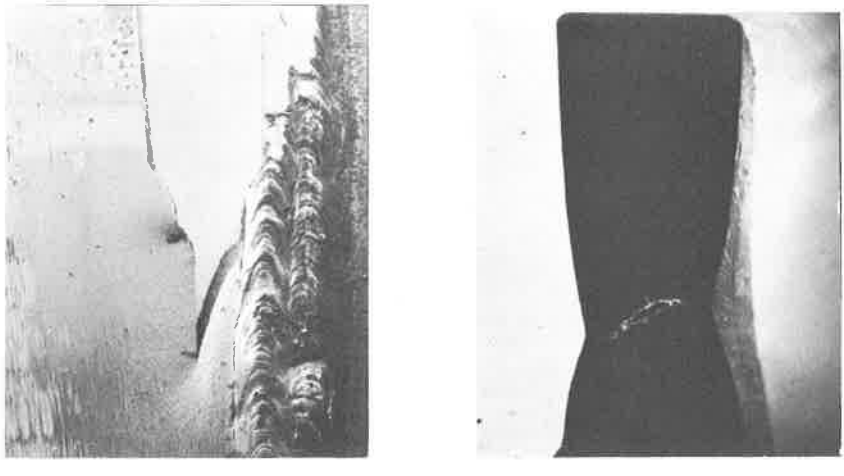

FIGURE 6: Reduction in area at the crack tip. No. 1.4948 (Type AISI 304) steel.